Lipid bilayer-coated mesoporous silica nanoparticles carrying bovine hemoglobin towards an erythrocyte mimic

Tu, J.; Bussmann, J.; Du, G.; Gao, Y.; Bouwstra, J.A.; Kros, A.

Lipid Bilayer-Coated Mesoporous Silica Nanoparticles Carrying Bovine Hemoglobin as an Erythrocyte Mimic

Jing Tu [1], Jeroen Bussmann [1, 2], Guangsheng Du [3], Yue Gao [1], Joke A. Bouwstra [3], Alexander Kros [1*]

[1]Department of Supramolecular & Biomaterials Chemistry, Leiden Institute of Chemistry (LIC), Leiden University, P.O. Box 9502, 2300 RA Leiden, The Netherlands

[2]Leiden Institute of Biology, Gorlaeus Laboratories, Leiden University, P.O. Box 9502, Leiden, 2300 RA, The Netherlands

[3]Division of Drug Delivery Technology, Cluster BioTherapeutics, Leiden Academic Centre for Drug Research (LACDR), Leiden University, P.O. Box 9502, 2300 RA Leiden, The Netherlands

*Corresponding Author.

Dr Alexander Kros: E-mail: a.kros@chem.leidenuniv.nl

Graphical Abstract

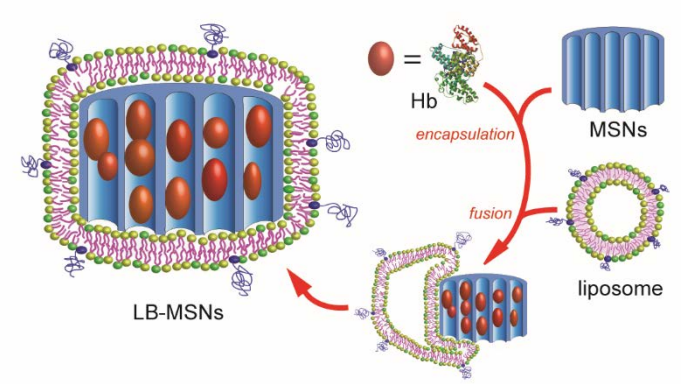

The formation of an erythrocyte mimic (lipid bilayer-coated mesoporous silica nanoparticles carrying bovine hemoglobin)

Abstract

Hemoglobin (Hb)-loaded mesoporous silica nanoparticles (MSNs) coated with a lipid bilayer (LB-MSNs) were investigated as an erythrocyte mimic. MSNs with a large average pore size (10 nm) act as a rigid core and provide a protective environment for Hb encapsulated inside the pores. The colloidal stability of Hb-loaded MSNs was enhanced upon the application of a lipid bilayer, through fusion of PEGylated liposomes onto the exterior surface of Hb-loaded MSNs. The morphology and mesostructure of the MSNs were characterized by scanning electron microscopy (SEM), transmission electron microscopy (TEM) and surface area analysis. The Hb loading capacity (mg/g) in MSNs was studied by thermogravimetric analysis (TGA). UV-Vis absorption spectroscopy revealed that Hb inside MSNs had an identical, but slightly broadened peak in the Soret region compared to free Hb. Furthermore the encapsulated Hb exhibits similar peroxidase-like activity in catalyzing the oxidation of 2,2′-azino-bis(3-ethylbenzothiazoline-6-sulfonic acid) diammonium salt (ABTS) with hydrogen peroxide. The introduction of a supported lipid bilayer (LB) demonstrated the potential to prevent premature Hb release (the burst release amount decreased from 25.50±0.33% to 6.73±0.83%) and increased the colloidal stability of the Hb-loaded MSNs (hydrodynamic diameter remained ~250 nm for at least one week). The *in vivo* systemic circulation and biodistribution of LB-MSNs were studied in optically transparent zebrafish embryos, revealing that LB-MSNs have the potential to act as an erythrocyte mimic in transfusion therapy.

Keywords: Mesoporous silica nanoparticles, Hemoglobin, Lipid bilayer, Zebrafish embryos, Erythrocyte mimic

1. Introduction

Due to the shortage of blood donations and the risks associated with allogenic donor blood transfusion, such as virus infection, and unmatched blood types, artificial red blood cell (RBC) substitutes have been investigated intensively during the past decades.(Duan et al., 2012; Klein et al., 2007; Wang et al., 2015) To mimic and fulfill some functions of RBCs, there are two main types of artificial RBC substitute in development.(Duan et al., 2012; Henkel-Honke and Oleck, 2007; Jia et al., 2016) Apart from perfluorocarbon emulsion-based substitutes,(Spahn, 1999) Hb (6.5 × 5.4 × 5.5 nm, Mw 64500)-based oxygen carriers (HBOC) have attracted increasing attention.(Jia et al., 2012; Jia et al., 2016; Shi et al., 2009; Urabe et al., 2007) Hb is the essential oxygen carrying protein in erythrocytes.(Liu et al., 2012) Pioneering work was performed with stroma-free Hb,(Chang, 2004, 2012; Chen et al., 2012; Duan et al., 2012; Tsuchida et al., 2009) which unfortunately was unsuitable because it induces side effects such as vasoconstriction and renal toxicity in mammals.(Li et al., 2005; Xiong et al., 2012; Zhao et al., 2007) Therefore several approaches have been explored to overcome these challenges, including nanocarriers such as lipid vesicles (Li et al., 2005; Yadav et al., 2016) and biodegradable polymers.(Lu et al., 2016; Rameez et al., 2008; Wang et al., 2017; Zhao et al., 2007) The emerged focus on the encapsulation of Hb into nanosized carriers (Gao et al., 2011; Jia et al., 2016) is because nanoparticle-based erythrocyte mimics offer several distinct advantages, including 1) prevention of vasoconstriction, 2) avoidance of renal toxicity, and 3) the protection of Hb from degradation in bodily fluids to prolong the circulation time.(Jia et al., 2016; Zhao et al., 2007)

Liposome-based carriers of Hb are one of the most important HBOC formulations and have been widely studied.(Gao et al., 2011; Li et al., 2005; Sakai et al., 2000) Liposome-encapsulated Hb with a size of 250 nm were proven to be safe and the elimination of vasoconstriction.(Gao et al., 2011; Sakai et al., 2004) However, liposomes are fragile and

easily deform when exposed to fluid shear stresses.(Li et al., 2005) Several strategies have been investigated to increase the liposome's mechanical strength, like using solid silica nanoparticle (diameter ~10 nm) as core for a rigid support,(Liu et al., 2012) introducing an actin matrix inside the aqueous core of submicron liposomes.(Li et al., 2005; Liu et al., 2012) MSNs can be used as protein delivery carriers due to their unique properties, namely biocompatibility, chemical inertness, large surface area and controllable pore size.(Liu et al., 2009a; Liu et al., 2009b; Liu et al., 2009c; Slowing et al., 2009) Inspired by nature, Brinker and others reported a versatile nanocarrier that synergistically integrates the advantages of liposomes with MSNs, resulting in LB coated MSNs with a so-called "protocell" structure (Scheme 1).(Ashley et al., 2011; Durfee et al., 2016; Liu et al., 2009a; Liu et al., 2009b; Liu et al., 2009c; Meng et al., 2015) The electrostatic interaction of zwitterionic liposomes with the negatively charged MSNs surface, results in vesicle rupture and concomitant bilayer formation. As a result, the MSNs pores are sealed and the cargo of interest encapsulated inside the MSNs.(Liu et al., 2009a; Liu et al., 2009c; Meng et al., 2015; Mornet et al., 2005) Furthermore, the lipid bilayer acts as an immune-isolative barrier, which can prevent recognition by the reticuloendothelial system and as a result enhance the circulation time.(Arifin and Palmer, 2003; Liu et al., 2016; Yadav et al., 2016) Recently, nanosized-MSNs with large pore diameters (10 nm) and therefore capable of accommodating Hb inside have been developed in our group. (Tu et al., 2016) To increase the colloidal stability under physiological conditions and biocompatibility, a LB was applied (LB-MSNs).(Bouchoucha et al., 2014) In addition, the charge-neutral highly hydrophilic polymer polyethylene glycol (PEG) was incorporated in the LB to induce stealth-like behavior.(Garay et al., 2012; Li et al., 2005; Tonga et al., 2014)

Herein, we demonstrate a facile method to prepare LB-MSNs as a potential oxygen carrier. MSNs with a 10 nm channel diameter are used to accommodate Hb. To improve the

colloidal stability of these Hb-loaded MSNs, a supported lipid bilayer was introduced to decorate the outer surface of Hb-loaded MSNs resulting in a core-shell structure. The preparation of these nanoparticles is schematically illustrated in Scheme 1. The presence of a lipid bilayer lowers the premature release of Hb. Circulation and distribution studies were performed in zebrafish embryos in order to investigate the *in vivo* behavior of the these lipid bilayer coated MSNs.

2. Experimental Section

2.1 Materials

Bovine hemoglobin (Hb, Mw~64500), Pluronic P123 ($EO_{20}PO_{70}EO_{20}$, M_n~5800), tetraethyl orthosilicate (TEOS, ≥98%), hydrochloric acid (HCl), 1,3,5-trimethylbenzene (TMB), 2',2'-azino-bis (3-ethylbenzothiazoline-6-sulfonic) acid (ABTS) and fluorescein isothiocyanate were purchased from Sigma-Aldrich and used as received. 1,2-dioleoyl-sn-glycero-3-phosphocholine (DOPC), 1,2-dioleoyl-sn-glycero-3-phosphoethanolamine (DOPE), 1,2-dioleoyl-sn-glycero-3-phosphoethanolamine-N-[methoxy(polyethylene glycol)-2000] (ammonium salt) ($PEG_{2000}PE$) and 1,2-dioleoyl-sn-glycero-3-phosphoethanolamine-N-(lissamine rhodamine B sulfonyl) (ammonium salt) (DOPE-LR) were purchased from Avanti Polar Lipids. Fluorocarbon surfactant FC-4 was purchased from Yick-Vic Chemicals & Pharmaceuticals (HK) Ltd. Sephadex G25 was purchased from GE Healthcare Life Sciences. The composition of the phosphate buffered saline (PBS) used was: K_2HPO_4 (14.99 mM), KH_2PO_4 (5 mM), and NaCl (150.07 mM), with an ionic strength of 270 mM, pH 7.4. The phosphate buffer (PB) with an ionic strength of 12 mM was prepared by mixing Na_2HPO_4 (1 mM) and NaH_2PO_4 (1 mM) at molar ratio of 5:2. Milli-Q water (18.2 MΩ/cm, Millipore Co., USA) was used throughout the experiment. All Hb solutions for the experiments were freshly

prepared before each experiment. Silicon wafers <110> dsp of 0.38 mm thickness, cut in pieces 1 by 1 cm were a kind gift from U-needle B.V.

2.2 Synthesis of large-pore MSNs

MSNs were synthesized as follows. (Tu et al., 2016) 0.5 g surfactant Pluronic P123 and 1.4 g of FC-4 were dissolved in 80 mL of HCl (0.02 M), followed by the introduction of 0.48 mL of TMB. After stirring for 6 h, 2.14 mL of TEOS was added dropwise. The resulting mixture was stirred at 30 ˚C for 24 h and transferred to an autoclave at 120 ˚C for 2 days. Finally, the solid product was isolated by centrifugation (4000 rpm, 10 min), and washed with ethanol and water. The organic template was completely removed by calcination at 550 ˚C for 5 h.

2.3 Preparation of liposome

Liposomes were prepared by dispensing stock solutions of DOPC (80 µl, 25 mg/mL), DOPE (40 µl, 25 mg/mL), and PEG2000-PE (30 µl, 25 mg/mL) into scintillation vials. All lipids were dissolved in chloroform. A lipid film was formed by slow evaporation of chloroform in the vial under a nitrogen flow and kept under vacuum overnight. The lipid film was rehydrated by the addition of phosphate buffer (2 mL, 1 mM, pH 7.4) and the mixture was vortexed to form a cloudy lipid suspension. The obtained suspension was sonicated in a water bath (50 °C, Branson 2510) for 10 min. If necessary, fluorescent lipids (DOPE-LR) were incorporated into the lipid mixture at 1 wt% to make fluorescent liposomes. The resulting liposomes were stored at 4 °C (final lipid concentration was 1.875 mg/mL).

2.4 Loading Hb into MSNs

MSNs were dispersed in phosphate buffer (PB, 1 mM, pH 7.4) at a concentration of 2 mg/mL and sonicated for 10 min using a low power sonication bath (Branson). 0.5 mL of MSNs were mixed with a series of Hb solutions with relatively low concentrations (solutions) and shaken using an Eppendorf mixer (400 rpm, 25 °C) for 10 min. Hb-loaded MSNs were collected by centrifugation (13000 rpm, 5 min) for further physical characterization and the amount of non-encapsulated Hb in the supernatant was quantified using a Tecan M1000 plate reader. A calibration curve was determined based on the absorbance at 405 nm as a function of Hb concentration (0-350 μg/mL).

The maximum loading capacity (mg/g) of Hb in MSNs can be obtained by thermogravimetric analysis (TGA),(Duan et al., 2012) the same loading procedure was repeated by mixing MSNs suspensions and Hb with higher initial concentrations (0, 0.25, 0.5, 1, 1.5, 2, 3 and 4 mg/mL). Before thermogravimetric analysis (TGA), Hb-loaded MSNs were freeze-dried until the weight was constant.

2.5 Preparation of LB-MSNs

To prepare LB-MSNs, 0.5 mL of Hb (0.5 mg/mL, 1 mM PB, pH 7.4) was transferred into a 2-mL Eppendorf tube, followed by the addition of a MSNs suspension (0.5 mL, 2 mg/mL). After shaking for 10 min, Hb-loaded MSNs were isolated by centrifugation (13000 rpm, 5 min). A dispersion (0.5 mL) of Hb-loaded MSNs (1 mg/mL) in PB (1 mM, pH 7.4) was mixed with 0.5 mL of as-prepared liposomes (composed of DOPC, DOPE, $PEG_{2000}PE$) and the mixture was shaken for 1.5 h (400 rpm, 25 °C). LB-MSNs were separated by centrifugation (13000 rpm, 5 min) from the excess of liposomes in the supernatant and then washed 3 times with PB. The hydrodynamic diameter and zeta-potential were determined as a function of time

for 1 week in 1 mM PB (pH 7.4) using a Malvern Nano-zs instrument. Hb-loaded MSNs (1:4 *w/w*) were used as control.

2.6 Characterization of MSNs, Hb-loaded MSNs and LB-MSNs

The morphology and mesostructure of the MSNs were characterized with scanning electron microscopy (SEM) and transmission electron microscopy (TEM). SEM imaging was conducted using a NovaSem microscope with an accelerating voltage of 15 kV and TEM imaging was conducted on a JEOL 1010 instrument with an accelerating voltage of 70 kV. Nitrogen adsorption-desorption isotherms were obtained with a Micromeritics TrisStar II 3020 surface area analyzer. Before the measurements, MSNs (at 300 °C) and Hb-loaded MSNs (at 25 °C) were outgassed in the instrument for 16 h under vacuum (< 0.15 mbar). The specific surface areas were calculated from the adsorption data in the low pressure range using the Brunauer-Emmett-Teller (BET) model.(Brunauer S. , 1938) The pore size distribution was determined following the Barrett-Joyner-Halenda (BJH) model.(Barrett et al., 1951) The hydrodynamic size distribution and polydispersity index (PDI), and zeta-potential were measured by dynamic light scattering (DLS) and laser doppler velocimetry, respectively, by using a Nano ZS® zetasizer (Malvern instruments, Worcestershire, U.K.). Thermogravimetric analysis (TGA) was conducted with a Perkin Elmer TGA7. All the samples were tested under an air atmosphere from 25 °C to 800 °C at a heating rate of 10 °C/min. UV-VIS absorbance spectra were measured using 96-well plates with a Tecan M1000 plate reader. A few drops of LB-MSNs (liposomes labelled with 1 wt% DOPE-LB and Hb labelled with FITC) suspension were added on silicon slide and dried prior to imaging. The fluorescence images were obtained using fluorescence microscopy (Zeiss Axio imager D2 fluorescence microscope, magnification 100×).

201

202 **2.7 Peroxidase-like activity of Hb-loaded MSNs and Hb**

203 The peroxidase-like activity of Hb after encapsulation by MSNs was measured
204 using 2',2'-azino-bis (3-ethylbenzothiazoline-6-sulfonic) acid (ABTS).(Slowing et al.,
205 2007; Urabe et al., 2007) An ABTS solution was prepared by dissolving 15 mg of
206 ABTS in 1 mL MilliQ water and 9 mL acetic acid.(Takayanagi and Yashiro, 1984)
207 Hydrogen peroxide (1 mL, 30% *w/w* in water) was diluted into 30 mL of MilliQ water.
208 Hb (0.05 and 0.1 mg/mL, 5 µl) and Hb-loaded MSNs (0.05 and 0.1 mg/mL, 5 µl) were
209 mixed with hydrogen peroxide (150 µL) in 96-well plate followed by the immediate
210 addition of the ABTS solution (45 µL). The absorbance at 418 nm of the oxidized
211 blue-green $ABTS^{\cdot+}$ was monitored every 20 sec for 20 min using a plate reader (Tecan
212 infinite M1000). The control experiment was performed by using enzyme-free PBS
213 and plain MSNs (0.05 and 0.1 mg/mL) in PBS. All experiments were performed in
214 triplicate.

215

216 **2.8 Labeling of Hb with Fluorescein isothiocyanate**

217 Hb (10 mg) was dissolved in 5 mL of sodium carbonate buffer (100 mM, pH 9).
218 Fluorescein isothiocyanate (FITC) was dissolved in DMSO at 1 mg/mL, and 0.25 mL
219 of the FITC solution was added to the protein solution. The mixture was stirred
220 overnight at 4 °C. The resulting FITC-labelled Hb was purified by size exclusion
221 chromatography using a Sephadex-G25 column and PBS as the eluent.

222

223 **2.9 Release profiles of Hb from MSNs and LB-MSNs**

224 The *in vitro* release profiles of Hb from MSNs and LB-MSNs were investigated
225 by suspending Hb-loaded MSNs or LB-MSNs in PBS (warmed to 37 °C, pH 7.4) at a

concentration of 1 mg/mL. The solution was incubated at 37 °C using an Eppendorf mixer (400 rpm). At various time points, the solution was centrifuged (13000 rpm, 5 min) and the supernatants were replaced with fresh PBS. The released amount of Hb in the supernatant was determined with a Tecan M1000 plate reader. All analyses were performed in triplicate.

2.10 Zebrafish husbandry

Transgenic zebrafish of the Tg (kdrl:GFP) strain, which has a GFP reporter gene expressed specifically in the endothelial cells,(Choi et al., 2007; Evensen et al., 2016) resulting in a green fluorescent vasculature. Zebrafish were handled in compliance with the local animal welfare regulations and maintained according to standard protocols (zfin.org). Embryos were raised in egg water (0.21 gm Instant Ocean sea salts in 1 liter of demi water) at 28.5 °C. For the duration of the lipid bilayer coated MSN injections, embryos were kept under anesthesia in egg water containing 0.02% buffered 3-aminobenzoic acid ethyl ester (Tricaine). The breeding of adult fish was approved by the local animal welfare committee (DEC) of the University of Leiden. All protocols adhered to the international guidelines specified by the EU Animal Protection Directive 2010/63/EU.

2.11 Zebrafish injection of LB-MSNs

A stock solution of LB-MSNs (5 mg/mL) and injected (5 μL) into the duct of cuvier. PBS injections were used as a control experiment. Injections were performed using a FemtoJet microinjector (Eppendorf) and a micromanipulator with pulled microcapillary pipettes.

2.12 Confocal microscopy imaging

Embryos were imaged after injection, embedded in 1% low melting point agarose and transferred to a Leica DMIRBE inverted microscope with a Leica SP1 confocal scan head for imaging with 40 or 63× lenses. For quantification purposes acquisition settings and area of imaging (in the caudal vein region) were kept the same across the groups.

2.13 Statistic analysis

All data shown are mean corrected values ± SD of at least three experiments.

3. Results and discussion

The morphology and mesoporous structure of the MSNs was analyzed by scanning electron microscopy (SEM) and transmission electron microscopy (TEM). From the SEM images, it became apparent that particles were non-spherical, the diameter of the as-prepared MSNs was found to be < 100 nm (Fig. 1a). The TEM images more clearly visualized that the particles were 90 ± 20 nm long, with an average width of 43 ± 7 nm (average of 150 nm particles) in line with previous reports.(Tu et al., 2016; Tu et al., 2017) TEM imaging also revealed that the particles possessed an array of disc-shaped mesochannels that run parallel to the short axis of the MSNs (Fig. 1b).

To characterize the channels within the cuboidal MSNs and to prove encapsulation of Hb molecules within the channels is possible, nitrogen sorption measurements were performed. Both MSNs and Hb-loaded MSNs, exhibited characteristic type IV isotherms with type H_1 hysteresis loops, revealing that these nanoparticles have disc-like mesopores according to International Union of Pure and Applied Chemistry (IUPAC) classification.(Zhang et al., 2014) The presence of encapsulated Hb does reduce the surface area from 506 m^2/g to 275 m^2/g. This is in agreement with the reduced average channel diameter from 10 nm (MSNs) to

7 nm (Hb-loaded MSNs), which was confirmed from the desorption branch of the isotherm using the Barrett-Joyner-Halenda (BJH) method (Fig. 1c,d). Thus upon Hb encapsulation both surface area and pore diameter of the MSNs decreased, indicating that hemoglobin was indeed encapsulated within the channels of the MSNs.

Thermogravimetric analysis (TGA) is one of most commonly use methods to detect the drug loading efficiency of inorganic nanoparticles.(Duan et al., 2012; Zhang et al., 2014; Zhang et al., 2010) Therefore, the percentage of Hb loaded within the MSNs was determined by TGA.(Duan et al., 2012) We observed that the weight loss upon heating the sample corresponding to the amount of Hb inside the MSNs for Hb correlated with the initial Hb concentration. Upon heating, both MSNs (as control) and MSNs/Hb (initial concentration, 4 mg/mL) underwent a total weight loss of 3.8% (H_1) and 42.1% (H_2) when measured up to 800 °C (Fig. 2a). The initial weight loss up to 100 °C was caused by the removal of thermo-desorbed water corresponding to 1.5% (L_1) and 3.4% (L_2) of the total weight loss. The weight loss (W) corresponding to Hb was calculated according to the following equation 1:(Xie et al., 2013)

$$\frac{H1-L1}{100-H1} = \frac{H2-W-L2}{100-H2}$$

$$W = H_2 - L_2 - \frac{(H1-L1)(100-H2)}{100-H1} \quad (1)$$

L: the initial weight loss until 100 °C was caused by the presence of thermo-desorbed water; H: the total weight loss up to 800 °C; Plain MSNs were used as control, L_1 (100 °C) and H_1 (800 °C).

The maximum loading capacity (37.3%) was obtained when the initial concentration of Hb used to load the MSNs was 4 mg/mL, (Fig. 2b). To investigate the encapsulation procedure in more detail, MSNs (2 mg/mL) were loaded with Hb using concentration range of this protein (0-700 µg/mL). This revealed that Hb loading in MSNs is linearly correlated (R^2 = 0.993) with the initial Hb concentration (0-700

μg/mL, Fig. 2c). At higher initial concentration of Hb this correlation is lost, presumably due to the blockage of pores of the MSNs with protein (Fig. 2b,c).

Hemoglobin can act as a peroxidase-like protein as its heme center catalyzes the reduction of hydrogen peroxide. Compared to inorganic catalysts, Hb has a high substrate specificity and reactive efficiency under normal conditions.(Urabe et al., 2007) To examine the enzymatic activity of encapsulated Hb, the oxidation of ABTS by hydrogen peroxide was used as an indicator.(Urabe et al., 2007) The catalytic reactivity of MSNs/Hb was analyzed and compared with native Hb in solution (Hb concentrations, 0.025 and 0.5 mg/mL). As shown in Fig. 3b,c, the kinetics of the two enzyme-catalyzed reactions are essentially identical, indicating that the encapsulated Hb in MSNs exhibit high peroxidase-like activity comparable to native Hb in aqueous solution.(Slowing et al., 2007) As expected, a higher concentration of Hb resulting a faster conversion of H_2O_2.

Next the heme protein folding was investigated by inspection of the Soret band in the UV-Visible absorption spectrum of hemoglobin as it is sensitive to the microenvironment, substructure, and oxidation state.(Xian et al., 2007) The spectral characteristics of MSNs/Hb (Hb concentration: 25-350 μg/mL) showed absorption curves that closely resembled those of native Hb as in all cases the maximum absorption was centered at 405 nm and no blue-shift was observed, suggesting no occurrence of protein unfolding.(Wu et al., 2013) The only noticeable difference is that MSNs/Hb showed some slight peak broadening, probably caused by the light scattering of MSNs (Fig. 3a,c). A good linear relationship (R^2 = 0.983) between the absorbance (405 nm) and MSNs/Hb concentration was obtained, similar to native Hb (Fig. 3b,d, R^2 = 0.999). This confirms that Hb retains its higher-order structure in the

mesopores of MSNs and does not undergo significant denaturation after encapsulation inside the silica pores.(Urabe et al., 2007; Xian et al., 2007)

Efficient encapsulation of Hb into MSNs occurs when the physicochemical properties of the Hb surface and the MSNs are complementary.(Hudson et al., 2008; Mathe et al., 2013) As the isoelectric point (pI) of Hb is 6.8-7.0 and 2-3 for the MSNs.(Gao et al., 2011; Hudson et al., 2008) both MSNs and Hb are negatively charged at physiological pH (7.4). The amount of Hb encapsulated in the MSNs was dependent on its initial concentration, indicating that the adsorption process was probably driven by capillary action.(Liu et al., 2011) Hb was encapsulated into the mesoporous channels (Fig. 1c,d), but also the encapsulation process on the outer surface of the MSNs (Fig. S1). At higher Hb concentrations, the hydrodynamic diameter of Hb-loaded MSNs increased dramatically due to aggregation (Fig. S1a). The long-term colloidal stability of LB-MSNs is an important criteria for future biomedical applications. Therefore a lipid bilayer was introduced to coat the Hb-loaded MSNs and form a physical barrier preventing colloidal aggregation resulting in LB-MSNs (Fig. 4a). The hydrodynamic diameter and the zeta-potential of LB-MSNs were measured as a function of time in order to study the long-term colloidal stability. The hydrodynamic diameter and the zeta-potential remained stable (~250 nm, ~-23 mV) for at least one week (Fig. 4b,c). Next, the cumulative release of Hb from MSNs and LB-MSNs was studied *in vitro* (Fig. 4d). Hb-loaded MSNs (1:4 *w/w*) showed a burst release during the first hour with a release amount of 25.50 ± 0.33%, while for LB-MSNs this was decreased to 6.73 ± 0.83%. After 180 h, the cumulative release of Hb-loaded MSNs and LB-MSNs was 42.27 ± 0.60% and 27.49 ± 0.29%, respectively. This shows that the lipid bilayer acts as a physical barrier lowering the amount of Hb leaking out from the MSNs (Fig. 4d).

Fluorescence microscopy imaging was used to visualize and confirm the localization of Hb within the nanoparticles using fluorescence light microscopy. For this study, Hb was labelled with fluorescein isothiocyanate (FITC) while the lipid lissamine rhodamine dye DOPE-LR was used to visualize the lipid bilayer on the Hb-loaded MSNs (Fig. S2). Due to the low magnification (100×) of the microscope and the small particle size (~250 nm, Fig. 4a,b), it was not possible to observe single particle in great detail. Despite of this, the overlap of both dyes is a clear indication of the co-localization of Hb and the lipid bilayer at the same particle. Furthermore, the uniform distribution of LB-MSNs on the silicon slide used as a substrate for imaging proved that the LB-MSNs were well-dispersed.

Finally a pilot in vivo study was performed in zebrafish (*Danio rerio*) embryos to study the circulation and distribution upon injection in the blood stream. Zebrafish embryos have emerged as an important transparent vertebrate model and are useful *in vivo* model for real-time imaging technique of a wide activity of biological processes and to study the distribution and circulation of nanoparticles.(Evensen et al., 2016; Sharif et al., 2012; White et al., 2008) To study the *in vivo* behaviour of hemoglobin loaded LB-MSNs in circulation, we injected fluorescent labelled LB-MSNs into the blood circulation system. After injection, the nanoparticles moved with the flow at high speed and readily distributed throughout the circulation of the bloodstream as evidenced by confocal imaging.(Evensen et al., 2016) (see Supporting Information movie 

MSNs_Flow.avi and Fig. 5).

Imaging revealed that LB-MSNs could systemic circulate and are evenly distributed in the blood vessels, with only little aggregation in the caudal hematopoietic tissue and the dorsal region of the yolk sac (Fig. 5). The large majority of the

nanoparticles did not interact with the endothelium as only a few adhered to the endothelium lining of the blood vessel and were trapped as expected. PEGylation of nanoparticle has shown to be an effective method to lower the binding affinity of the particles for endothelial cells *in vivo*.(Evensen et al., 2016) However, further optimization of the lipid bilayer composition and the amount of PEGylation are planned.

4. Conclusion

In summary, lipid bilayer coated MSNs were used as a carrier for hemoglobin for the first time. The large disc-like pores (10 nm) of the MSNs enabled the rapid encapsulation of Hb into the mesopores with a high loading capacity. Encapsulated Hb remained active and exhibited similar enzymatic activity to non-encapsulated Hb. The introduction of a supported lipid bilayer prevented premature Hb release from LB-MSNs and improved the colloidal stability *in vitro*. Therefore these Hb loaded LB-MSNs could be considered as an artificial erythrocyte mimic. The circulation and distribution of the LB-MSNs was tested in zebrafish embryos revealing that these nanoparticles remain in circulation upon injection, which is a critical property for any succesful erythrocyte mimic. Unfortunately, convective blood flow is not essential to supply oxygen to the tissues during the early larval development of zebrafish.(Grillitsch et al., 2005) Therefore Hb oxygen transport had no effect on oxygen-dependent processes (Pelster and Burggren, 1996) as even mutant zebrafish lacking erythrocytes survive for about 2 weeks after fertilization.(Grillitsch et al., 2005; Weinstein et al., 1996) While zebrafish embryos have emerged as a fast, cheap and relevant *in vivo* model for pre-screening of nanomedicine formulations(Brittijn et al., 2009; Kiene et al., 2017; Sharif et al., 2012; Sieber et al., 2017; Yang et al., 2016),

399 further evaluations using other animal models (*e.g.* mice) are required to test these Hb-
400 loaded MSNs as a true erythrocyte mimic. Furthermore, to perform all three functions
401 of erythrocyte, LB-MSNs load Hb, together with antioxidant enzymes (catalase and
402 dismutase) and carbonic anhydrase will be fabricated and evaluated in the future.
403

404 **Acknowledgements**

405 JT acknowledges the support from the Chinese Scholarship Council. JB acknowledges
406 the support of the NWO via a VENI grant. Alexander V. Korobko assisted with BET
407 measurements in Delft University of Technology. Dr. Aimee Boyle is thanked for her
408 critical reading of this manuscript. Shuxin Yang and Herman P. Spaink are thanked for
409 zebrafish culture.
410

411 **Supporting Information**

412 The supporting information contains hydrodynamic diameter of Hb-loaded MSNs and
413 fluorescent images of LB-MSNs on the silicon slides, the movement and distribution of
414 nanoparticles throughout the circulation of the bloodstream.
415

416 **References**

417 Arifin, D.R., Palmer, A.F., 2003. Determination of size distribution and encapsulation
418 efficiency of liposome-encapsulated hemoglobin blood substitutes using asymmetric flow
419 field-flow fractionation coupled with multi-angle static light scattering. Biotechnol. Prog
420 19, 1798-1811.
421 Ashley, C.E., Carnes, E.C., Phillips, G.K., Padilla, D., Durfee, P.N., Brown, P.A., Hanna,
422 T.N., Liu, J., Phillips, B., Carter, M.B., Carroll, N.J., Jiang, X., Dunphy, D.R., Willman,
423 C.L., Petsev, D.N., Evans, D.G., Parikh, A.N., Chackerian, B., Wharton, W., Peabody,
424 D.S., Brinker, C.J., 2011. The targeted delivery of multicomponent cargos to cancer cells
425 by nanoporous particle-supported lipid bilayers. Nat. Mater. 10, 389-397.
426 Barrett, E.P., Joyner, L.G., Halenda, P.P., 1951. The Determination of Pore Volume and Area
427 Distributions in Porous Substances .1. Computations from Nitrogen Isotherms. J. Am.
428 Chem. Soc. 73, 373-380.

Bouchoucha, M., C-Gaudreault, R., Fortin, M.A., Kleitz, F., 2014. Mesoporous Silica Nanoparticles: Selective Surface Functionalization for Optimal Relaxometric and Drug Loading Performances. Adv. Funct. Mater. 24, 5911-5923.

Brittijn, S.A., Duivesteijn, S.J., Belmamoune, M., Bertens, L.F.M., Bitter, W., De Bruijn, J.D., Champagne, D.L., Cuppen, E., Flik, G., Vandenbroucke-Grauls, C.M., Janssen, R.A.J., De Jong, I.M.L., De Kloet, E.R., Kros, A., Meijer, A.H., Metz, J.R., Van der Sar, A.M., Schaaf, M.J.M., Schulte-Merker, S., Spaink, H.P., Tak, P.P., Verbeek, F.J., Vervoordeldonk, M.J., Vonk, F.J., Witte, F., Yuan, H.P., Richardson, M.K., 2009. Zebrafish development and regeneration: new tools for biomedical research. Int. J. Dev. Biol. 53, 835-850.

Brunauer S. , E.P.H., Teller E., 1938. Adsorption of Gases in Multimolecular Layers. J. Am. Chem. Soc. 60, 309-319.

Chang, T.M.S., 2004. Hemoglobin-based red blood cell substitutes. Artif. Organs 28, 789-794.

Chang, T.M.S., 2012. From artificial red blood cells, oxygen carriers, and oxygen therapeutics to artificial cells, nanomedicine, and beyond. Artif. Cells, Blood Substitutes, Biotechnol. 40, 197-199.

Chen, K., Merkel, T.J., Pandya, A., Napier, M.E., Luft, J.C., Daniel, W., Sheiko, S., DeSimone, J.M., 2012. Low modulus biomimetic microgel particles with high loading of hemoglobin. Biomacromolecules 13, 2748-2759.

Choi, J., Dong, L., Ahn, J., Dao, D., Hammerschmidt, M., Chen, J.N., 2007. FoxH1 negatively modulates flk1 gene expression and vascular formation in zebrafish. Dev. Biol. 304, 735-744.

Duan, L., Yan, X.H., Wang, A.H., Jia, Y., Li, J.B., 2012. Highly Loaded Hemoglobin Spheres as Promising Artificial Oxygen Carriers. ACS Nano 6, 6897-6904.

Durfee, P.N., Lin, Y.S., Dunphy, D.R., Muniz, A.J., Butler, K.S., Humphrey, K.R., Lokke, A.J., Agola, J.O., Chou, S.S., Chen, I.M., Wharton, W., Townson, J.L., Willman, C.L., Brinker, C.J., 2016. Mesoporous Silica Nanoparticle-Supported Lipid Bilayers (Protocells) for Active Targeting and Delivery to Individual Leukemia Cells. ACS Nano, 8325-8345.

Evensen, L., Johansen, P.L., Koster, G., Zhu, K., Herfindal, L., Speth, M., Fenaroli, F., Hildahl, J., Bagherifam, S., Tulotta, C., Prasmickaite, L., Maelandsmo, G.M., Snaar-Jagalska, E., Griffiths, G., 2016. Zebrafish as a model system for characterization of nanoparticles against cancer. Nanoscale 8, 862-877.

Gao, W., Sha, B.Y., Zou, W., Liang, X., Meng, X.Z., Xu, H., Tang, J., Wu, D.C., Xu, L.X., Zhang, H., 2011. Cationic amylose-encapsulated bovine hemoglobin as a nanosized oxygen carrier. Biomaterials 32, 9425-9433.

Garay, R.P., El-Gewely, R., Armstrong, J.K., Garratty, G., Richette, P., 2012. Antibodies against polyethylene glycol in healthy subjects and in patients treated with PEG-conjugated agents. Expert Opin. Drug Delivery 9, 1319-1323.

Grillitsch, S., Medgyesy, N., Schwerte, T., Pelster, B., 2005. The influence of environmental P(O(2)) on hemoglobin oxygen saturation in developing zebrafish Danio rerio. J. Exp. Biol. 208, 309-316.

Henkel-Honke, T., Oleck, M., 2007. Artificial oxygen carriers: a current review. J. Am. Assoc. Nurse Anesth. 75, 205-211.

Hudson, S., Cooney, J., Magner, E., 2008. Proteins in mesoporous silicates. Angew. Chem., Int. Ed. 47, 8582-8594.

Jia, Y., Cui, Y., Fei, J.B., Du, M.C., Dai, L.R., Li, J.B., Yang, Y., 2012. Construction and Evaluation of Hemoglobin-Based Capsules as Blood Substitutes. Adv. Funct. Mater. 22, 1446-1453.

Jia, Y., Duan, L., Li, J., 2016. Hemoglobin-Based Nanoarchitectonic Assemblies as Oxygen Carriers. Adv. Mater. 28, 1312-1318.

Kiene, K., Schenk, S.H., Porta, F., Ernst, A., Witzigmann, D., Grossen, P., Huwyler, J., 2017. PDMS-b-PMOXA Polymersomes for Hepatocyte Targeting and Assessment of Toxicity. Eur. J. Pharm. Biopharm.

Klein, H.G., Spahn, D.R., Carson, J.L., 2007. Transfusion Medicine 1-Red blood cell transfusion in clinical practice. Lancet 370, 415-426.

Li, S.L., Nickels, J., Palmer, A.F., 2005. Liposome-encapsulated actin-hemoglobin (LEAcHb) artificial blood substitutes. Biomaterials 26, 3759-3769.

Liu, J., Jiang, X., Ashley, C., Brinker, C.J., 2009a. Electrostatically Mediated Liposome Fusion and Lipid Exchange with a Nanoparticle-Supported Bilayer for Control of Surface Charge, Drug Containment, and Delivery. J. Am. Chem. Soc. 131, 7567-7569.

Liu, J.W., Stace-Naughton, A., Brinker, C.J., 2009b. Silica nanoparticle supported lipid bilayers for gene delivery. Chem. Commun., 5100-5102.

Liu, J.W., Stace-Naughton, A., Jiang, X.M., Brinker, C.J., 2009c. Porous Nanoparticle Supported Lipid Bilayers (Protocells) as Delivery Vehicles. J. Am. Chem. Soc. 131, 1354-1360.

Liu, M.X., Gan, L.H., Chen, L.H., Zhu, D.Z., Xu, Z.J., Hao, Z.X., Chen, L.W., 2012. A novel liposome-encapsulated hemoglobin/silica nanoparticle as an oxygen carrier. Int. J. Pharm. 427, 354-357.

Liu, X., Zhu, L., Zhao, T., Lan, J., Yan, W., Zhang, H., 2011. Synthesis and characterization of sulfonic acid-functionalized SBA-15 for adsorption of biomolecules. Microporous Mesoporous Mater. 142, 614-620.

Liu, X.S., Situ, A., Kang, Y.A., Villabroza, K.R., Liao, Y.P., Chang, C.H., Donahue, T., Nel, A.E., Meng, H., 2016. Irinotecan Delivery by Lipid-Coated Mesoporous Silica Nanoparticles Shows Improved Efficacy and Safety over Liposomes for Pancreatic Cancer. ACS Nano 10, 2702-2715.

Lu, M., Zhao, C., Wang, Q., You, G., Wang, Y., Deng, H., Chen, G., Xia, S., Zhao, J., Wang, B., Li, X., Shao, L., Wu, Y., Zhao, L., Zhou, H., 2016. Preparation, characterization and in vivo investigation of blood-compatible hemoglobin-loaded nanoparticles as oxygen carriers. Colloids Surf., B 139, 171-179.

Mathe, C., Devineau, S., Aude, J.C., Lagniel, G., Chedin, S., Legros, V., Mathon, M.H., Renault, J.P., Pin, S., Boulard, Y., Labarre, J., 2013. Structural determinants for protein adsorption/non-adsorption to silica surface. PLoS One 8, e81346.

Meng, H., Wang, M., Liu, H., Liu, X., Situ, A., Wu, B., Ji, Z., Chang, C.H., Nel, A.E., 2015. Use of a Lipid-Coated Mesoporous Silica Nanoparticle Platform for Synergistic Gemcitabine and Paclitaxel Delivery to Human Pancreatic Cancer in Mice. ACS Nano, 3540-3557.

Mornet, S., Lambert, O., Duguet, E., Brisson, A., 2005. The formation of supported lipid bilayers on silica nanoparticles revealed by cryoelectron microscopy. Nano Lett. 5, 281-285.

Pelster, B., Burggren, W.W., 1996. Disruption of hemoglobin oxygen transport does not impact oxygen-dependent physiological processes in developing embryos of zebra fish (Danio rerio). Circ. Res. 79, 358-362.

Rameez, S., Alosta, H., Palmer, A.F., 2008. Biocompatible and biodegradable polymersome encapsulated hemoglobin: a potential oxygen carrier. Bioconjugate Chem. 19, 1025-1032.

Sakai, H., Horinouchi, H., Masada, Y., Takeoka, S., Ikeda, E., Takaori, M., Kobayashi, K., Tsuchida, E., 2004. Metabolism of hemoglobin-vesicles (artificial oxygen carriers) and their influence on organ functions in a rat model. Biomaterials 25, 4317-4325.

Sakai, H., Tomiyama, K., Sou, K., Takeoka, S., Tsuchida, E., 2000. Poly(ethylene glycol)-conjugation and deoxygenation enable long-term preservation of hemoglobin-vesicles as oxygen carriers in a liquid state. Bioconjugate Chem. 11, 425-432.

Sharif, F., Porta, F., Meijer, A.H., Kros, A., Richardson, M.K., 2012. Mesoporous silica nanoparticles as a compound delivery system in zebrafish embryos. Int. J. Nanomed. 7, 1875-1890.

Shi, Q., Huang, Y., Chen, X., Wu, M., Sun, J., Jing, X., 2009. Hemoglobin conjugated micelles based on triblock biodegradable polymers as artificial oxygen carriers. Biomaterials 30, 5077-5085.

Sieber, S., Grossen, P., Detampel, P., Siegfried, S., Witzigmann, D., Huwyler, J., 2017. Zebrafish as an early stage screening tool to study the systemic circulation of nanoparticulate drug delivery systems in vivo. J. Controlled Release 264, 180-191.

Slowing, I.I., Trewyn, B.G., Lin, V.S.Y., 2007. Mesoporous silica nanoparticles for intracellular delivery of membrane-impermeable proteins. J. Am. Chem. Soc. 129, 8845-8849.

Slowing, I.I., Wu, C.W., Vivero-Escoto, J.L., Lin, V.S.Y., 2009. Mesoporous Silica Nanoparticles for Reducing Hemolytic Activity Towards Mammalian Red Blood Cells. Small 5, 57-62.

Spahn, D.R., 1999. Blood substitutes artificial oxygen carriers: perfluorocarbon emulsions. Crit. Care 3, R93-R97.

Takayanagi, M., Yashiro, T., 1984. Colorimetry of Hemoglobin in Plasma with 2,2'-Azino-Di(3-Ethylbenzthiazoline-6-Sulfonic Acid) (Abts). Clin. Chem. 30, 357-359.

Tonga, G.Y., Saha, K., Rotello, V.M., 2014. 25th Anniversary Article: Interfacing Nanoparticles and Biology: New Strategies for Biomedicine. Advanced Materials 26, 359-370.

Tsuchida, E., Sou, K., Nakagawa, A., Sakai, H., Komatsu, T., Kobayashi, K., 2009. Artificial Oxygen Carriers, Hemoglobin Vesicles and Albumin-Hemes, Based on Bioconjugate Chemistry. Bioconjugate Chem. 20, 1419-1440.

Tu, J., Boyle, A.L., Friedrich, H., Bomans, P.H.H., Bussmann, J., Sommerdijk, N.A.J.M., Jiskoot, W., Kros, A., 2016. Mesoporous Silica Nanoparticles with Large Pores for the Encapsulation and Release of Proteins. ACS Appl. Mater. Interfaces 8, 32211-32219.

Tu, J., Du, G., Reza Nejadnik, M., Monkare, J., van der Maaden, K., Bomans, P.H.H., Sommerdijk, N., Slutter, B., Jiskoot, W., Bouwstra, J.A., Kros, A., 2017. Mesoporous Silica Nanoparticle-Coated Microneedle Arrays for Intradermal Antigen Delivery. Pharm. Res. 34, 1693-1706.

Urabe, Y., Shiomi, T., Itoh, T., Kawai, A., Tsunoda, T., Mizukami, F., Sakaguchi, K., 2007. Encapsulation of hemoglobin in mesoporous silica (FSM)-enhanced thermal stability and resistance to denaturants. Chembiochem 8, 668-674.

Wang, Q., Zhang, R., Lu, M., You, G., Wang, Y., Chen, G., Zhao, C., Wang, Z., Song, X., Wu, Y., Zhao, L., Zhou, H., 2017. Bioinspired Polydopamine-Coated Hemoglobin as Potential Oxygen Carrier with Antioxidant Properties. Biomacromolecules 18, 1333-1341.

Wang, W.Q., Liu, S., Huang, Y.B., Jing, X.B., Xie, Z.G., 2015. Biodegradable dextran vesicles for effective haemoglobin encapsulation. J. Mater. Chem. B 3, 5753-5759.

Weinstein, B.M., Schier, A.F., Abdelilah, S., Malicki, J., SolnicaKrezel, L., Stemple, D.L., Stainier, D.Y.R., Zwartkruis, F., Driever, W., Fishman, M.C., 1996. Hematopoietic mutations in the zebrafish. Development 123, 303-309.

White, R.M., Sessa, A., Burke, C., Bowman, T., LeBlanc, J., Ceol, C., Bourque, C., Dovey, M., Goessling, W., Burns, C.E., Zon, L.I., 2008. Transparent adult zebrafish as a tool for in vivo transplantation analysis. Cell Stem Cell 2, 183-189.

Wu, J., Li, X., Yan, Y., Hu, Y., Zhang, Y., Tang, Y., 2013. Protein adsorption onto nanozeolite: effect of micropore openings. J. Colloid Interface Sci. 406, 130-138.

577 Xian, Y., Xian, Y., Zhou, L., Wu, F., Ling, Y., Jin, L., 2007. Encapsulation hemoglobin in
578 ordered mesoporous silicas: Influence factors for immobilization and bioelectrochemistry.
579 Electrochem. Commun. 9, 142-148.
580 Xie, M., Shi, H., Li, Z., Shen, H.J., Ma, K., Li, B., Shen, S., Jin, Y., 2013. A multifunctional
581 mesoporous silica nanocomposite for targeted delivery, controlled release of doxorubicin
582 and bioimaging. Colloids Surf., B 110, 138-147.
583 Xiong, Y., Steffen, A., Andreas, K., Muller, S., Sternberg, N., Georgieva, R., Baumler, H.,
584 2012. Hemoglobin-based oxygen carrier microparticles: synthesis, properties, and in vitro
585 and in vivo investigations. Biomacromolecules 13, 3292-3300.
586 Yadav, V.R., Rao, G., Houson, H., Hedrick, A., Awasthi, S., Roberts, P.R., Awasthi, V., 2016.
587 Nanovesicular liposome-encapsulated hemoglobin (LEH) prevents multi-organ injuries in
588 a rat model of hemorrhagic shock. Eur. J. Pharm. Sci. 93, 97-106.
589 Yang, J., Shimada, Y., Olsthoorn, R.C.L., Snaar-Jagalska, B.E., Spaink, H.P., Kros, A., 2016.
590 Application of Coiled Coil Peptides in Liposomal Anticancer Drug Delivery Using a
591 Zebrafish Xenograft Model. ACS Nano 10, 7428-7435.
592 Zhang, X.X., Li, F.F., Guo, S.Y., Chen, X., Wang, X.L., Li, J., Gan, Y., 2014.
593 Biofunctionalized polymer-lipid supported mesoporous silica nanoparticles for release of
594 chemotherapeutics in multidrug resistant cancer cells. Biomaterials 35, 3650-3665.
595 Zhang, Y., Zhi, Z., Jiang, T., Zhang, J., Wang, Z., Wang, S., 2010. Spherical mesoporous
596 silica nanoparticles for loading and release of the poorly water-soluble drug telmisartan. J.
597 Controlled Release 145, 257-263.
598 Zhao, J., Liu, C.S., Yuan, Y., Tao, X.Y., Shan, X.Q., Sheng, Y., Wu, F., 2007. Preparation of
599 hemoglobin-loaded nano-sized particles with porous structure as oxygen carriers.
600 Biomaterials 28, 1414-1422.
601

602

603

604 **Scheme 1.** Procedure for the formation of LB-MSNs. (a) Encapsulation of Hb into the MSNs,
605 followed by fusion of (b) liposome (composed of DOPC/DOPE/PEG_{2000}PE), resulting in (c)
606 LB-MSNs (*i.e.* protocell).

607

608 **Fig. 1.** (a, b) SEM and TEM images of MSNs. Scale bar = 250 nm. (c) Nitrogen adsorption-
609 desorption isotherms and (d) plots of pore diameter vs. pore volume, calculated from the
610 desorption isotherms using the BJH model, show that the MSNs and Hb loaded MSNs (146
611 mg/g) have an average pore diameter of 10 ± 1 nm and 7.5 ± 1.5 nm, respectively.

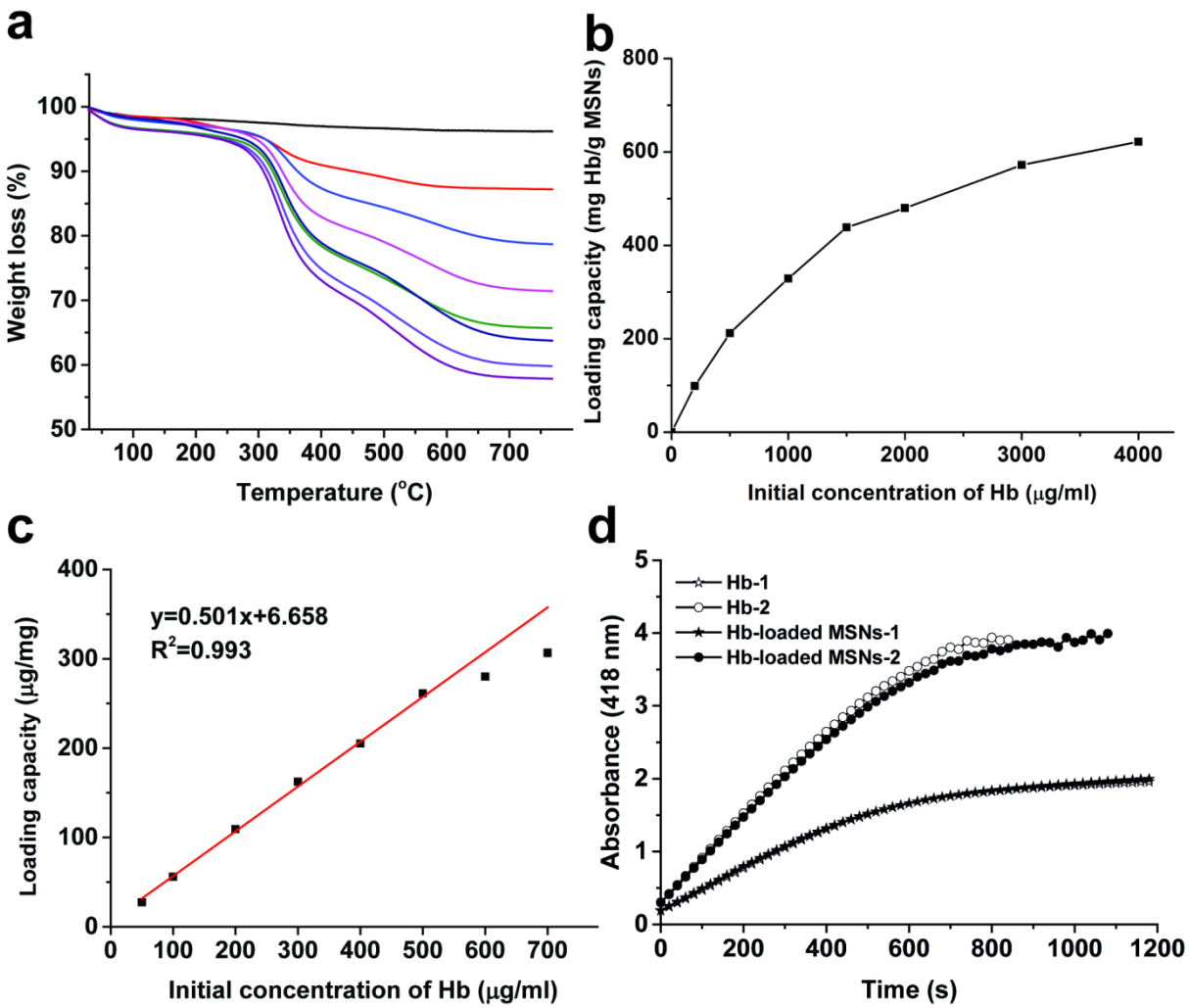

612

613

614 **Fig. 2.** (a) TGA curves of Hb-loaded MSNs with different initial concentrations of Hb (0, 0.25,
615 0.5, 1, 1.5, 2, 3 and 4 mg/mL, from top to bottom) and its corresponding b) LC of Hb into
616 MSNs calculated by TGA; (c) Loading capacity of Hb into MSNs at low loading
617 concentrations by a Tecan M1000 plate reader, absorbance at 405 nm, 0-700 μg/mL); (d)
618 ABTS catalyzed by native Hb (white) and MSNs/Hb (black). Hb_{-1} and Hb-loaded $MSNs_{-1}$
619 represent the initial concentration of Hb were 50 μg/mL and Hb_{-2} and Hb-loaded $MSNs_{-2}$
620 were 100 μg/mL. The enzymatic activity of Hb was measured at 418 nm by examining the
621 catalytic conversion of the oxidation of ABTS.

622

Fig. 3. (a) UV-VIS absorption spectra of Hb at varying concentrations (25-350 μg/mL), 1 mM PB as a control; (b) standard curve of Hb absorbance (405 nm); (c) UV-VIS absorption spectra of Hb-loaded MSNs with varying concentration (based on Hb, 25-350 μg/mL), 1 mg/mL MSNs in 1 mM PB as a control; (d) standard curve of Hb-loaded MSNs (405 nm).

Fig. 4. Colloidal stability of LB-MSNs. (a) Hydrodynamic diameter of MSNs and LB-MSNs according to DLS (1 mM PB, pH 7.4); (b) size stability (insert: PDI values) and (c) zeta-potential of LB-MSNs were measured as a function of time (1 mM PB, pH 7.4) at room temperature, (mean ± SD, n =3); (d) release profiles of Hb-loaded MSNs and LB-MSNs in PBS (37 °C, pH 7.4), (mean ± SD, n =3).

Fig. 5. Confocal fluorescence images of (a) lissamine rhodamine labeled LB-MSNs), with a few regular red dots attributed to autofluorescence, (b) GFP expressed blood vessels of a zebrafish embryo, (c) overlay images show the localization of the LB-MSNs in the blood vessels.